Insights into the Molecular Basis for the Carbenicillinase Activity of PSE-4 β-Lactamase from Crystallographic and Kinetic Studies†

Daniel Lim,‡ François Sanschagrin,§ Lori Passmore,‡ Liza De Castro,‡ Roger C. Levesque,§ and Natalie C. J. Strynadka*,‡

Department of Biochemistry and Molecular Biology, University of British Columbia, Vancouver, British Columbia, Canada, V6T 1Z3, and Laboratoire de Génie Génétique, Département de Microbiologie, Faculté de Médecine, Université Laval, Quebec, Canada, G1K 7P4

Received July 17, 2000; Revised Manuscript Received October 6, 2000

ABSTRACT: PSE-4 is a class A β-lactamase produced by strains of *Pseudomonas aeruginosa* and is highly active for the penicillin derivative carbenicillin. The crystal structure of the wild-type PSE-4 carbenicillinase has been determined to 1.95 Å resolution by molecular replacement and represents the first structure of a carbenicillinase published to date. A superposition of the PSE-4 structure with that of TEM-1 shows a rms deviation of 1.3 Å for 263 Cα atoms. Most carbenicillinases are unique among class A β-lactamases in that residue 234 is an arginine (ABL standard numbering scheme), while in all other class A enzymes this residue is a lysine. Kinetic characterization of a R234K PSE-4 mutant reveals a 50-fold reduction in k_{cat}/K_m and confirms the importance of Arg 234 for carbenicillinase activity. A comparison of the structure of the R234K mutant refined to 1.75 Å resolution with the wild-type structure shows that Arg 234 stabilizes an alternate conformation of the Ser 130 side chain, not seen in other class A β-lactamase structures. Our molecular modeling studies suggest that the position of a bound carbenicillin would be shifted relative to that of a bound benzylpenicillin in order to avoid a steric clash between the carbenicillin α-carboxylate group and the conserved side chain of Asn 170. The alternate conformation of the catalytic Ser 130 in wild-type PSE-4 may be involved in accommodating this shift in the bound substrate position.

β-Lactam antibiotics inhibit the penicillin binding proteins (PBPs) of bacteria, which catalyze the cross-linking of peptidoglycan. Inhibition of this reaction results in the formation of weakened cell walls in growing bacteria and ultimately leads to cell lysis. The most common resistance mechanism in bacteria against β-lactam compounds is the production of β-lactamases, periplasmic enzymes that hydrolyze and inactivate β-lactams (*1*−*3*). On the basis of their primary sequences, β-lactamases can be grouped into four classes: A, B, C, and D. The class B enzymes are metalloenzymes that require one or two zinc cations for activity. The class A, C, and D enzymes are serine hydrolases. The class C enzymes are primarily chromosomally encoded and are active against cephalosporins. Members of class D are penicillinases that are uniquely able to hydrolyze oxacillins. Clinically the most prevalent β-lactamases are the class A enzymes, which are mainly penicillinases, but point mutations in the TEM and SHV enzymes have increased the substrate spectrum of class A β-lactamases to include cephalosporins. The class A enzymes are 29 KDa proteins that are found in both Gram-negative and Gram-positive bacteria and can be either plasmid or chromosomally encoded.

PSE-4 is a class A β-lactamase (*4*) produced by certain strains of *Pseudomonas aeruginosa*, a Gram-negative opportunistic pathogen that has become a significant problem in hospitals worldwide (*5*). PSE-4 and other carbenicillinases are classified as group 2c β-lactamases (*7*) and show activity toward the penicillin derivative (*6*) carbenicillin (Figure 1) equal to or higher than that for aminopenicillins (*4*, *7*). Carbenicillin was first introduced in 1967 and was able to safely and effectively combat *P. aeruginosa* infections; however, resistance was soon reported (*9*). PSE-4 was first isolated from the carbenicillin-resistant strain Dalgleish in 1969 (*10*, *11*) and is the most commonly occurring β-lactamase in carbenicillin-resistant strains of *P. aeruginosa* (*4*). PSE-4 is closely related to a number of other carbenicillinases: PSE-1, CARB-3, and CARB-4 from *P. aeruginosa* (*12*−*16*), AER-1 from *Aeromonas hydrophila* (*16*), CARB-5 from *Acinetobacter calcoaceticus* var. anitratus (*17*), CARB-6 from *Vibrio cholerae* (*18*), GN79 and N29 from *Proteus mirabilis* (*19*, *20*), and PSE-3 from *Rhodopseudomonas capsulata* sp. 108 (*21*).

Residue 234 is arginine in all carbenicillinases sequenced to date (*4*, *13*−*20*) with the exception of PSE-3 (*21*) and AER-1 (*16*), which, like other class A β-lactamases, have lysine at this residue. The ABL standard numbering scheme for class A β-lactamases will be used throughout (*22*).

† Supported by an operating grant from the Medical Research Council (Canada) to N.C.J.S. and R.L. and by the Burroughs Wellcome Fund and Howard Hughes Medical Institute (to N.C.J.S.).

* To whom correspondence should be addressed.

‡ University of British Columbia. Phone: 604-822-0789. Fax: 604-822-5227.

§ Université Laval. Phone: 418-656-3070. Fax: 418-656-7176.

[1] Abbreviations: ABL, class A β-lactamase (standard numbering scheme); EDTA, ethylenediaminetetraacetic acid; IPTG, isopropyl β-D-thiogalactopyranoside; MOPS, 3-morpholinopropanesulfonic acid; PSE, *Pseudomonas* specific enzyme; PBP, penicillin binding protein; rms, root mean square; SDS, sodium dodecyl sulfate; Tris, tris(hydroxymethyl)-aminomethane.

[2] The coordinates for the wild-type and R234K mutant PSE-4 structures have been deposited in the Protein Data Bank with the accession codes 1G68 and 1G6A, respectively.

10.1021/bi001653v CCC: $20.00
Published on Web 12/14/2000

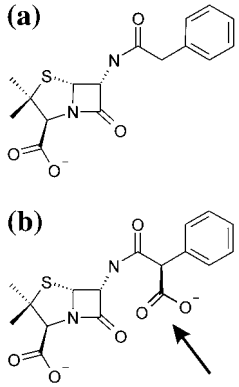

FIGURE 1: Structures of penicillin G (a) and carbenicillin (b). Carbenicillin contains an additional carboxylate at the α position indicated by the arrow.

Residue 234 is located within the binding pocket near the nucleophilic Ser 70. Previous molecular modeling studies have suggested that Arg 234 in PSE-4 may be involved in substrate recognition (*4*). Mutagenesis studies in the class A enzyme TEM-1 have also implicated a role for the K234R substitution in the hydrolysis of α-carboxypenicillins (*23*, *24*) in addition to other residues conserved in carbenicillinases. To clarify the role of the conserved arginine in carbenicillinases and to identify other structural features important for carbenicillinase activity, we have initiated crystallographic studies of the PSE-4 enzyme. The 1.95 Å wild-type structure and the structure of a R234K mutant refined to 1.75 Å presented here provide the first structural data on a carbenicillinase. Our kinetic and structural analyses of the wild-type and R234K mutant enzymes reveal unique features in PSE-4 that are likely important for carbenicillin hydrolysis.

MATERIALS AND METHODS

Enzyme Purification. The PSE-4 enzymes were expressed from pET30a-based constructs in *Escherichia coli* strain BL21 2DE3. The K234R PSE-4 mutant was obtained with the replacement mutagenesis method (*25*) using the following primer: 5′-GCCAGCACCTGAGCGATCCGCAATGTTCCA-3′.

The cells were grown in Aharonowitz medium (*26*) with 1 g of glycerol, 2.5 g of Casamino acid (Sigma), and 128 mg of ampicillin per liter. A 20 mL overnight culture was first pelleted by centrifugation and resuspended in 1 mL of fresh medium. The washed cells were then used to inoculate four 1 L cultures. The cultures were grown at 37 °C with vigorous shaking to an optical density (A_{600}) of approximately 0.5. The cultures were then induced with 1 mM IPTG and grown for an additional 4 h at room temperature.

Both mutant and wild-type PSE-4 enzymes were purified using an osmotic shock protocol, followed by anion exchange chromatography and gel filtration. The cells were pelleted, resuspended in 80 mL of 20% sucrose in 33 mM Tris, pH 8, with 1 mM EDTA, and incubated at room temperature for 10 min. The cells were then pelleted and resuspended in 40 mL of ice cold deionized H_2O with vigorous shaking and vortexing. After incubation on ice for 10 min, the cells were centrifuged at 5000*g* for 15 min. The supernatant was then further centrifuged at 20000*g* for 30 min. Stock buffer solution (1 M Tris, pH 8) was added to the supernatant to a final concentration of 30 mM.

Table 1: X-ray Data Statistics

	wild-type	R234K
space group	$P4_12_12$	
temperature (K)	100	
resolution (Å)[a]	25−1.95 (2.02−1.95)	25−1.75 (1.81−1.75)
observations	208 439	162 602
unique reflections[a]	21 494	29 406
completeness (%)[a]	99.5 (96.5)	99.5 (98.6)
average $I/\sigma(I)$[a]	33.0 (8.3)	25.4 (3.4)
$R_{sym}(I)$[a,b]	0.059 (0.219)	0.056 (0.359)

[a] Values in parentheses correspond to the highest resolution shell. [b] $R_{sym} = \sum|I_{av} - I_i|/\sum I_i$, where I_{av} is the average of all observations, I_i.

All protein purification was carried out at 4 °C. The sample was loaded at 2 mL/min onto a Q-sepharose FF (Pharmacia) column (1.5 cm × 10 cm) preequilibrated with 20 mM Tris, pH 8. The column was then washed overnight with 800 mL of the same buffer at 1 mL/min. This washing step improved the purity of the subsequently eluted fractions. The protein was eluted with a linear gradient of 0−200 mM NaCl at 1 mL/min over a volume of 100 mL. Protein concentration in the eluate was monitored by UV absorbance at 280 nm. Peak fractions were analyzed by SDS-PAGE. Fractions with the highest purity were pooled and concentrated to 0.5 mL by ultrafiltration (Millipore Ultrafree-15, 5 KDa MWCO). The sample was then loaded on to a sephacryl-100 column (3 cm × 80 cm) preequilibrated with 150 mM NaCl in 50 mM Tris, pH 8. The protein was eluted at 0.8 mL/min, and peak fractions with the highest purity as shown by SDS-PAGE were pooled, concentrated to 0.5 mL, and filtered through a 0.1 μm filter. Final protein concentration was determined by measuring UV absorbance at 280 nm in 6 M guanidine hydrochloride using an extinction coefficient of 1.031 cm^{-1} for a 1 mg/mL solution as estimated from the mature amino acid sequence (Expasy ProtParam web page [*27*, *28*]). Approximately 15 mg of enzyme was obtained from 4 L of culture.

Crystallization. Bipyramidal crystals of wild-type PSE-4 measuring up to 0.6 mm in length were grown using the hanging drop vapor diffusion method by mixing 3 μL of a 10 mg/mL protein solution with 1 μL of well solution consisting of 2 M ammonium sulfate, 50 mM MOPS, pH 6.4, and 100 mM $MgCl_2$. Crystals appeared after 1−2 days and grew to maximum size after 1−2 weeks at room temperature. The R234K mutant crystals were grown in a similar manner but with 0.1 M sodium acetate, pH 4.5, as the buffer. A qualitative test with nitrocefin showed that residual wild-type PSE-4 enzyme in the mother liquor was enzymatically active.

X-ray Data Collection. Data were collected at 100 K (Oxford Cryostream) with an *R*-axis IIc detector mounted on a Rigaku RU-200 X-ray generator (50 kV, 100 mA) with Osmic focusing mirrors. Crystals were cryoprotected by stepwise transfer to a solution of 2 M ammonium sulfate and 35% sucrose and mounted on the goniometer while blocking the cryostream. The data were processed using the HKL package (*29*) and programs from the CCP4 software suite (*30*). The statistics are summarized in Table 1. On the basis of systematic absences, the crystals belonged to either space group $P4_12_12$ or $P4_32_12$ with unit cell dimensions (wild-type) of $a = b = 95.157$ Å and $c = 62.793$ Å and one molecule per asymmetric unit with a V_M of 2.45 $Å^3$/Da (*31*).

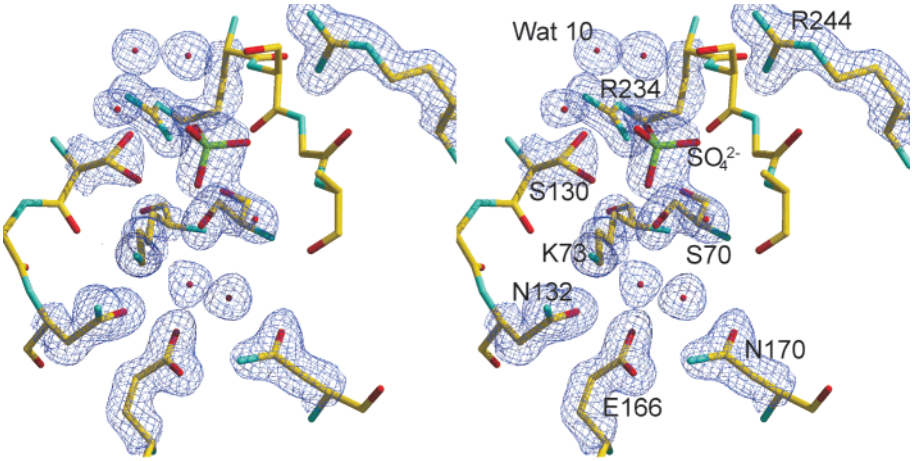

FIGURE 2: Representative SigmaA-weighted $2F_o - F_c$ electron density (*37*) in the active site region contoured at 1.5 σ and to a resolution of 1.95 Å. This figure was created with XtalView (*38*) and Raster3D (*56*). Unless otherwise stated, all other figures were created with Molscript (*57*) and Raster3D.

Enzyme Kinetics. Kinetics were measured at 30 °C in 50 mM sodium phosphate buffer, pH 7.0, in a 1 mL cuvette reaction volume with a Cary 1 spectrophotometer (Varian, Mississauga, Ont.). Hydrolysis for ampicillin ($\epsilon = 912$ M^{-1} cm^{-1}) and carbenicillin ($\epsilon = 1190$ M^{-1} cm^{-1}) was monitored at 232 nm. Penicillin G ($\epsilon = 546$ M^{-1} cm^{-1}) was monitored at 240 nm. Kinetic parameters V_{max} and K_m were determined by rates of hydrolysis calculated from the initial velocity in the linear portion, with the same cuvette and a least-squares calculation. The concentration of wild-type PSE-4 was 3.2 nM for the ampicillin and carbenicillin assays and 3.6 nM for the penicillin G assay. The concentrations of R234K mutant PSE-4 were 40, 500, and 10 nM for the assays with ampicillin, carbenicillin, and penicillin G, respectively. Concentrations of the substrates tested varied from 10 to 500 μM. All experiments were carried out in triplicate. Analysis of enzyme kinetic data was done with the Leonora software for robust regression analysis of enzyme data and a bi-weighting regression system (*32*). The values for the wild-type enzyme with carbenicillin and ampicillin were obtained from a previous study (*33*).

RESULTS

Structure Determination. The structure was determined by molecular replacement with the program AMoRe (*34*), using data from 15 to 4 Å and an integration radius of 25 Å. A search model was constructed from the TEM-1 native structure (*35*), which shares 44% sequence identity with PSE-4. Side chains in the TEM-1 structure were altered with the program O (*36*) to match the wild-type PSE-4 sequence and were manually adjusted to sterically favorable conformations. A rotation search yielded a top solution with a correlation coefficient of 14.0%, which led to a convincing translation solution in space group $P4_12_12$ (but not in $P4_32_12$) with a correlation coefficient of 37.4% and an *R*-factor of 50.1%. These scores were improved to 53.6% and 45.1%, respectively, after rigid body refinement.

Structure Refinement. On the basis of difference densities in the initial electron density maps calculated with the phases from the TEM-1 molecular replacement solution, the model was manually corrected using O (*36*). The model was then subjected to iterative cycles of refinement in the program CNS (*37*) and manual fitting with the program XFIT in the XtalView suite (*38*). Each refinement cycle consisted of positional minimization, simulated annealing, and individual *B*-factor refinement using a maximum likelihood target and data from 25 to 1.95 Å. Water molecules were added with the automated waterpicking protocol in CNS and manually inspected for reasonable hydrogen-bonding geometry and electron density. The final model includes all atoms from residues 24 to 290, 300 waters, and a sulfate anion. The sulfate group was positioned between Ser 130 and Arg 243 in the active site region to account for density that could not be modeled with any other known component of the crystallization conditions (Figure 2). The *B*-factors for the sulfate atoms were initially fixed at 17.7 $Å^2$ as estimated from the Wilson plot (*30*). The occupancy of the sulfate group was then refined to 0.47, following which the *B*-factors of the sulfate atoms were refined individually to a range of 22.4−28.1 $Å^2$. Significant residual density remained around the sulfate atoms, which was not readily interpretable. The model refined to an overall *R*-factor of 0.167 with a free *R*-factor of 0.213 and shows good stereochemistry with no residues in the disallowed regions of the Ramachandran plot (*39*).

The refined model of the wild-type enzyme (protein atoms only) and with Arg 234 replaced by alanine was used for initial refinement against the R234K data. After rigid body refinement, simulated annealing, and individual *B*-factor refinement, difference density for the Lys 234 side chain was clearly visible and unambiguously modeled. Refinement was completed after inclusion of 258 waters and a sulfate anion (modeled similarly as the sulfate in the wild-type structure). The rms deviation from the wild-type structure is 0.30 Å for all protein atoms (2035 pairs). The refinement statistics for the wild-type and R234K mutant structures are summarized in Table 2.

DISCUSSION

Overall Structure. The overall structure of PSE-4 is similar to those of other class A β-lactamases and consists of an α/β domain and a predominantly α-helical domain (Figure 3). The α/β domain contains a central five-stranded antiparallel β-sheet with α-helices on both sides. The active site is located at the interface between the two domains. The program ALIGN (*40*) was used to superimpose the Cα trace

Table 2: Structure Refinement Statistics

crystallographic *R*-factor[a]	0.167	0.177
free *R*-factor[b]	0.212	0.210
rms deviations from ideality		
bond lengths (Å)	0.0075	0.0097
bond angles (deg)	1.3	1.4
angle improper (deg)	0.87	0.97
average *B*-factor (Å^2)	20.2	20.9
no. of non-hydrogen atoms (protein/solvent/sulfate)	2057/300/5	2050/258/5

[a] Crystallographic *R*-factor, $R = \sum||F_o|_{(h,k,l)} - |F_c|_{(h,k,l)}|/\sum|F_o|_{(h,k,l)}$, where $|F_o|$ is observed structure factor amplitude, $|F_c|$ is the calculated structure amplitude from the model, and (h,k,l) are the reflection indices. Data in the full resolution range were used for refinement with no Σ cutoff. [b] Calculated from 5% of reflections excluded from refinement.

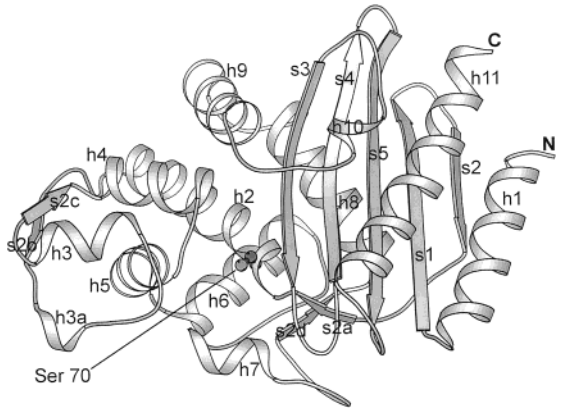

FIGURE 3: Overall structure of PSE-4. α-Helices are labeled from h1 to h11, while *β*-strands are labeled from s1 to s5. The active site is indicated by a ball-and-stick representation of the Ser 70 side chain.

of PSE-4 with those of other class A enzymes: *Streptomyces albus* G (*41*), *Enterobacter cloacae* NMC-A (*42*), *Escherichia coli* (strain TUH12191) TOHO-1 (*43*), *Klebsiella pneumoniae* SHV-1 (*44*), *Staphylococcus aureus* PC1 (*45*), *Bacillus licheniformis* 749/C (*46*), and *E. coli* TEM-1 (*35*) *β*-lactamases. The program identified equivalent Cα atoms using a structure-based alignment, for which the rms deviations are given in Table 4. A comparison of the Cα trace of PSE-4 with that of TEM-1 shows significant deviations at regions distant from the active site (the N- and C-termini, residues 50−59, residues 87−91, residues 226−230, and residues 251−258). Differences are also observed at residues 97−103 and 110−116, which are located on the helix−loop region adjacent to the substrate binding pocket. However, the core structure including the substrate binding cavity is well conserved (Figure 4a).

Active Site. The positions and orientations of the conserved catalytic residues in the wild-type PSE-4 structure are similar to those of other class A *β*-lactamases and consist of Ser 70 (nucleophile), Lys 73 (potential general base for acylation [*35*, *47*]), Ser 130 (proton transfer between the thiazolidine N4 and Lys 73), Glu 166 (possible general base for acylation or deacylation [*35*, *48*]), Asn 170 (coordination of deacylating water), and Arg 234 (depression of Ser 130 pK_a). A superposition of these residues with the corresponding residues in native TEM-1 shows a rms deviation of 0.4 Å for 47 pairs of main chain and side chain atoms (Figure 4b).

Small but significant differences between PSE-4 and the other class A penicillinases center around interactions from the unique Arg 234. The Arg 234 side chain is hydrogen-bonded to Wat 10 and the side chain hydroxyl of Ser 130. Ser 130 in the wild-type PSE-4 structure is uniquely observed in two alternate conformations (Figures 2 and 4b), which were each modeled with 50% occupancy. The *B*-factors for the two conformers both refined to 14.9 Å^2. In all other class A *β*-lactamase structures, the conformation of the Ser 130 side chain is such that the χ_1 values are in the range of −120.5° to −163.5° (−153.4° in PSE-4). The alternate conformer of the Ser 130 side chain ($\chi_1 = -69.7°$) in PSE-4 is stabilized by hydrogen-bonding to the Nη_1 and Nη_2 atoms of Arg 234 with distances of 3.0 and 2.9 Å, respectively.

Relative to Lys 234 in other class A *β*-lactamases, Arg 234 in wild-type PSE-4 is restricted in its ability to hydrogen bond with substrate, as hydrogen bonds are only favorable in the plane of the arginine guanidium group (Figures 2 and 4b). It therefore seems unlikely that the reduction in carbenicillinase activity by the R234K mutation in PSE-4 results from loss of substrate interactions with Arg 234. This is consistent with our kinetic data, which shows that the R234K mutation has little effect on the K_m for carbenicillin (Table 3). This also agrees with the crystal structure of the TEM-1−penicillin G acyl-enzyme intermediate, which showed that Lys 234 also makes only a minor electrostatic contribution to substrate binding (*35*).

The wild-type and R234K mutant PSE-4 structures differ only in the local region of residue 234, with the remainder of the protein being essentially unchanged (Figure 5a). Weaker density is seen for Wat 10 in the mutant structure (26.7 Å^2), which likely results from replacement of the Arg 234 Nϵ by the Lys 234 Cδ. The loss of the Arg 234 Nη_2 creates a void in the R234K PSE-4 mutant that is filled by Wat 52 (*B*-factor = 19.7 Å^2), which is not present in the wild-type structure. Relative to Lys 234 in other class A structures, the conformation of Lys 234 in the R234K PSE-4 mutant is unusual (Figure 5b) and positions the side chain Nζ atom further away from the active site so that it is hydrogen-bonded to the backbone oxygen of Thr 126 (2.9 Å) and Wat 52 (2.7 Å). It is not clear from the available structural data what factors stabilize the unusual conformation of Lys 234 in the PSE-4 R234K mutant, although it does not seem to result from the presence of Wat 52. Wat 52 is

Table 3: Effect of R234K Mutation on *β*-Lactam Hydrolysis

	wild-type[a]			R234K		
	K_m (μM)	K_{cat} (s^{-1})	K_{cat}/K_m ($\times 10^6$ s^{-1} M^{-1})	K_m (μM)	K_{cat} (s^{-1})	K_{cat}/K_m ($\times 10^6$ s^{-1} μM^{-1}) [relative to wild-type]
carbenicillin	68 ± 4	1200 ± 120	17 ± 2	129 ± 62	57 ± 11	0.4 ± 0.2 [0.02]
ampicillin	33 ± 3	1170 ± 130	35 ± 5	74 ± 11	840 ± 70	11 ± 2 [0.3]
penicillin G	57 ± 8	890 ± 40	16 ± 2	100 ± 40	430 ± 70	4 ± 2 [0.25]

[a] Values for carbenicillin and ampicillin hydrolysis (wild-type) were obtained from an earlier study (*33*).

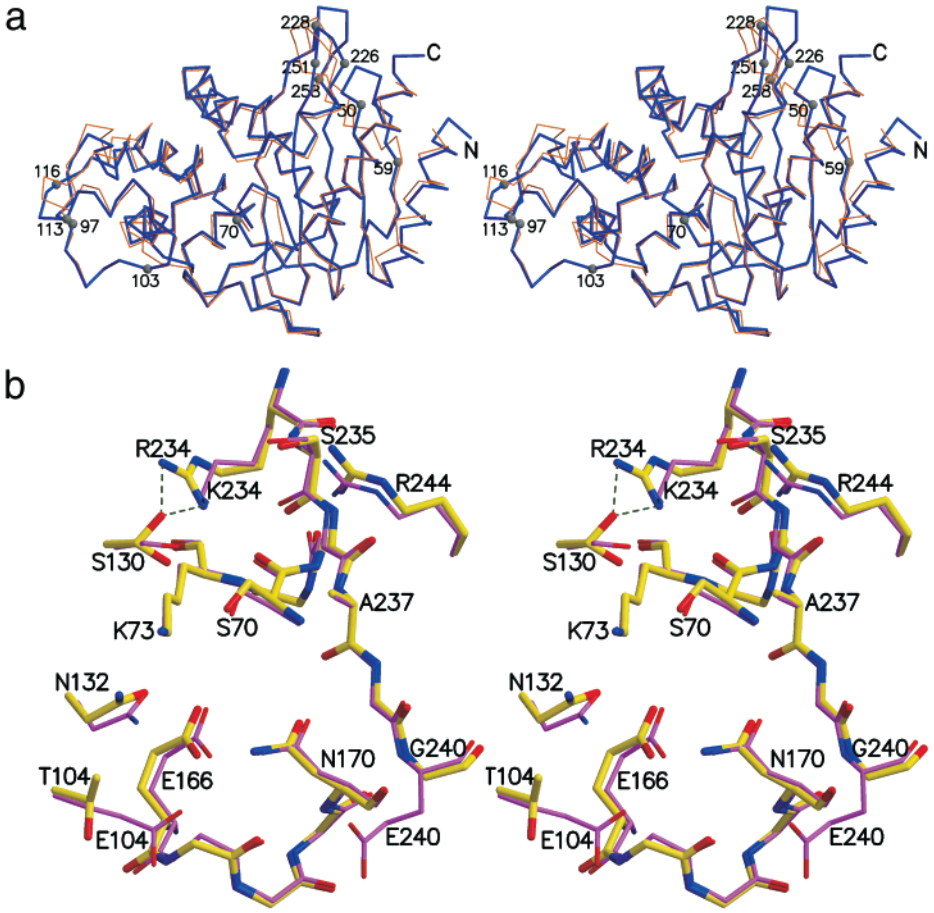

FIGURE 4: Comparison of the PSE-4 and TEM-1 structures. (a) Superposition of the Cα atoms of PSE-4 (thick trace) and TEM-1 (thin trace). The rms deviation for 261 pairs of Cα atoms is 1.27 Å. Residues 50−58, 226−228, and 250−256 show the largest deviations. Ser 70 indicates the location of the active site. (b) Superposition of the active sites of wild-type PSE-4 (thick rendering) and TEM-1 (thin rendering).

Table 4: Superposition of Wild-Type PSE-4 with Other Class A β-Lactamase Structures

	PBD code	no. of Cα atoms aligned	rms deviations (Å)
S. albus G	1BSG	257	2.1
NMC-A	1BUE	257	2.2
TOHO-1	1BZA	255	2
SHV-1	1SHV	264	1.9
PC1	3BLM	249	2.7
749/C	4BLM	253	2
TEM-1	ref *35*	261	1.3

not hydrogen-bonded to any other atom and therefore does not provide any bridging interactions that would help to anchor the Lys 234 Nζ. The conformation and hydrogen-bonding pattern of Lys 234 in the R234K PSE-4 mutant seems possible in other class A structures but is apparently not favored.

Lys 234 in the R234K PSE-4 mutant may still act to lower the pK_a of Ser 130, since the Lys 234 Nζ to Ser 130 Oγ distance (3.0 Å) is still within the range observed in other class A structures (2.6−3.0 Å). Interestingly, the side chain of Ser 130 in the R234K PSE-4 mutant is in a single conformation ($\chi_1 = -146.6°$, *B*-factor = 19.6 Å^2), the most significant structural difference resulting from the R234K substitution in PSE-4.

Model of the Acyl-Enzyme Intermediate. To visualize the relevance of the Ser 130 alternate conformer in carbenicillin hydrolysis, the acyl-enzyme intermediate of PSE-4 with carbenicillin was modeled using the TEM-1−penicillin G complex structure (Figure 6). The penicillin G atoms were positioned into the active site of PSE-4 by superimposing the TEM-1 Ser 70 atoms onto those of PSE-4. A carboxylate group was then added to the Cα atom of penicillin G, using an ideal model of carbenicillin (*50*) as a guide. The resulting model shows the carbenicillin α-carboxylate in a steric clash with the Asn 170 Nδ_2 (1.7 Å), a highly conserved residue in class A β-lactamases. The Asn 170 side chain forms a hydrogen-bonding network (observed in the vast majority of class A structures to date) with the side chain carboxylate of the proposed general base for deacylation, Glu 166, and the proposed deacylating water. Disruption of this hydrogen-bonding network is energetically unfavorable and would displace or eliminate the proposed deacylating water. Elimination of this water in an N170Q mutant of the PC1 β-lactamase reduced the steady-state rate of nitrocefin hydrolysis by 800-fold (*51*). Thus, the α-carboxylate of carbenicillin cannot be accommodated simply by movement of the Asn 170 side chain, and the position of carbenicillin in the PSE-4 substrate binding cavity is likely shifted relative to penicillin G in TEM-1. Given that Ser 130 is the only residue in a position to act as a proton donor to the substrate thiazolidine N4 during the acylation step (*35*), the alternate conformation of Ser 130 in wild-type PSE-4 may accommodate the shifted position of the carbenicillin thiazolidine N4.

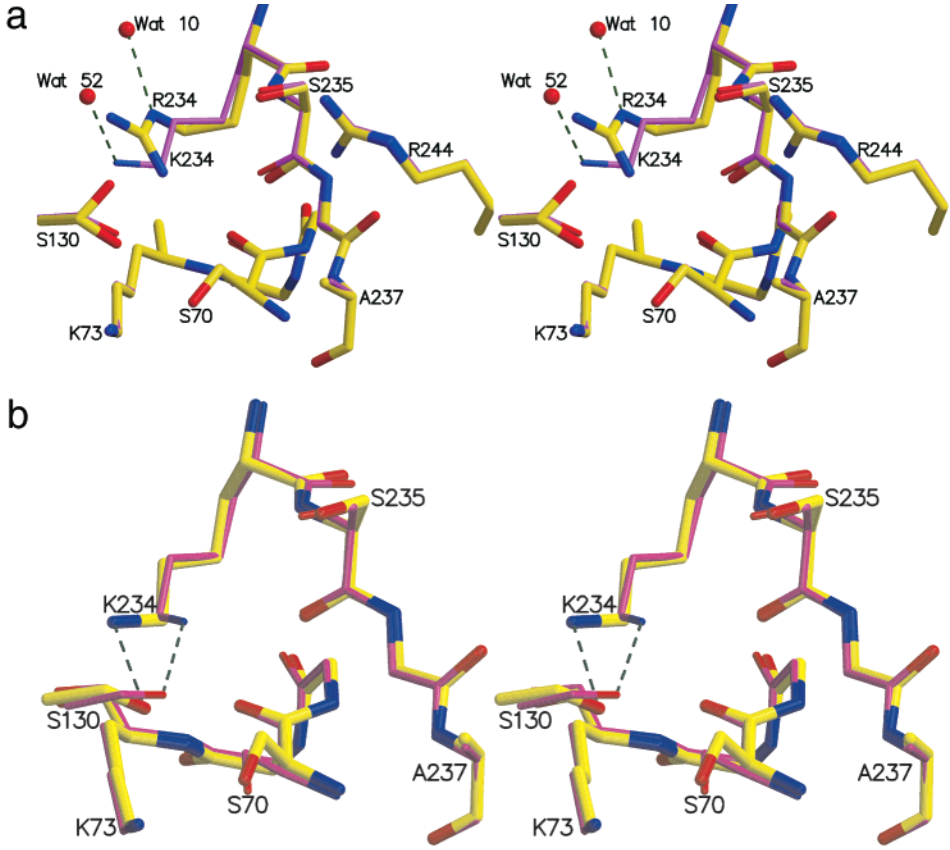

FIGURE 5: Comparison of the active site region of the R234K PSE-4 mutant with the wild-type PSE-4 and TEM-1 structures. (a) Superposition of the active site region near residue 234 of the wild-type (thick rendering) and R234K mutant (thin rendering) PSE-4 structures. Density for Wat 10 is markedly reduced in the R234K mutant structure. Wat 52 is only seen in the R234K mutant. (b) Superposition of the active site region near residue 234 of the R234K PSE-4 mutant (thick rendering) and TEM-1 (thin rendering). The position of the TEM-1 Lys 234 Nζ atom is similar to those of other class A β-lactamases.

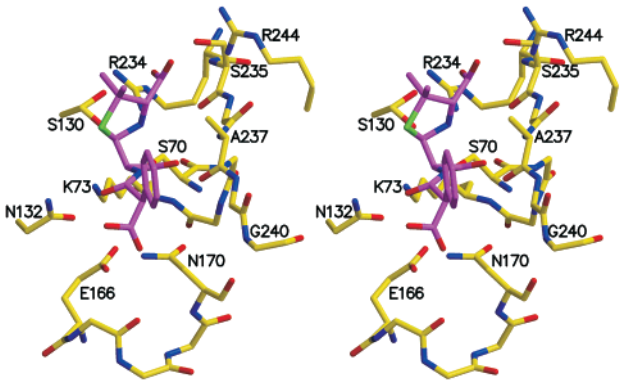

FIGURE 6: Model of the acyl-enzyme intermediate of PSE-4 with carbenicillin. The carbenicilloyl moiety is shown with purple carbons. The α-carboxylate is in a steric clash with Asn 170.

Similar to both the wild-type and R234K mutant PSE-4 enzymes (Table 3), TEM-1 exhibits comparable K_m values for benzylpenicillin and carbenicillin (24 and 14 μM, respectively [*24*]). The low rates of carbenicillin hydrolysis (relative to those for benzylpenicillin) for TEM-1 and the R234K PSE-4 mutant are largely due to low k_{cat} values. In the case of TEM-1, the k_{cat} for benzylpenicillin (1200 s^{-1}) and carbenicillin (120 s^{-1}) differed by an order of magnitude (*24*). That for these enzymes the rate of carbenicillin hydrolysis seems to be more dependent on turnover rate rather than on substrate affinity is consistent with the conformation of Ser 130 being the key difference between the wild-type and R234K mutant PSE-4 structures.

Kinetic studies of a K234R TEM-1 mutant, which showed a 6-fold increase in k_{cat} for carbenicillin with essentially no change in the k_{cat} for benzypenicillin, confirmed the importance of Arg 234 in catalyzing carbenicillin hydrolysis (*24*). However, increases in the K_m values for carbenicillin (13-fold) and benzylpenicillin (10-fold) indicate that the K234R substitution in TEM-1 resulted in changes in the substrate binding pocket that impaired overall substrate binding (*24*). Differences between the TEM-1 and PSE-4 structures must account for the inability of TEM-1 to fully accommodate an arginine at residue 234. Indeed, these differences may even involve residues distant from the active site, as was found to be the case with trypsin, for which mutations outside of the active site and S1 regions were necessary to introduce partial chymotrypsin activity (*52*). Given that certain structural features important for carbenicillinase activity may be very subtle, directed evolution (*53*, *54*) may provide an efficient means to identify mutations in TEM-1 that would confer high levels of carbenicilliase activity, particularly for positions distant from the active site and for which the contributions are less apparent from crystal structures. Such an approach was successful in isolating a TEM-1 triple mutant with a greater than 2000-fold increase in k_{cat}/K_m for cefotaxime (*55*). PSE-3 and AER-1 do not contain the K234R substitution and provide further examples of the importance of other factors for carbenicillinase activity. It will be

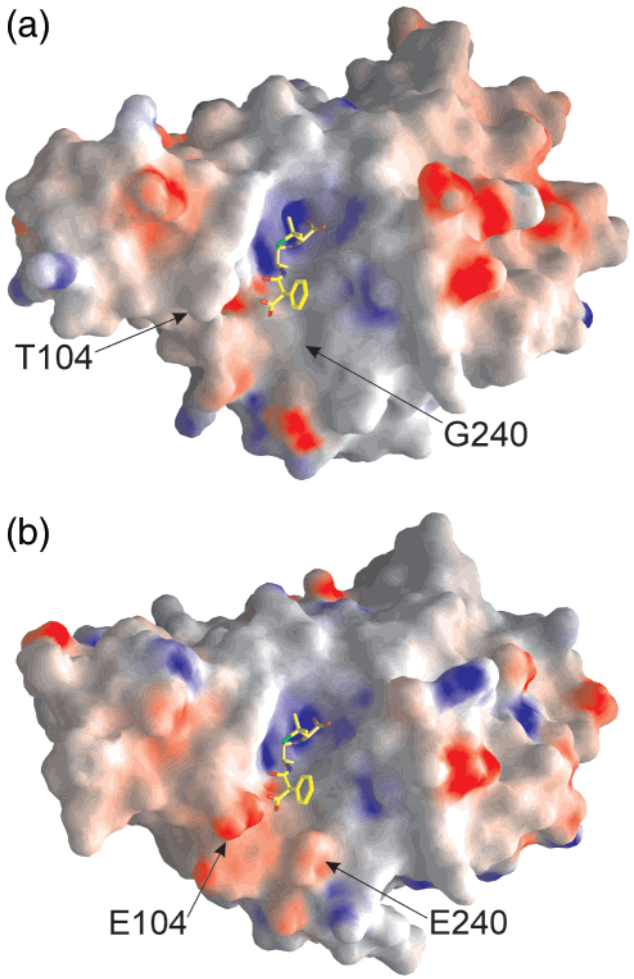

FIGURE 7: Comparison of the electrostatic surfaces of PSE-4 (a) and TEM-1 (b). Carbenicillin is shown in stick rendering with yellow carbon atoms. Negatively charged areas are shown in red, positively charged areas in blue, and neutral areas in gray. This figure was prepared with GRASP (*58*).

interesting to see if alternate conformations of Ser 130 are also present in the K234R TEM-1 mutant, and perhaps in PSE−3 and AER-1, in which an alternate conformer of Ser 130 may be stabilized in a different way.

Thr 104 and Gly 240 are conserved in all carbenicillinases (*4*, *13*−*19*), with the exception of PSE-3, in which residue 104 is proline and residue 240 is serine (*21*). The conservation of these residues suggested a role for Thr 104 and Gly 240 in carbenicillin hydrolysis or binding. The analogous residues in TEM-1 are negatively charged (Glu 104 and Glu 240) and thus may disfavor carbenicillin binding due to charge repulsion with the α-carboxylate group (Figures 4b and 7). However, the side chain carboxylates of both Glu 104 and Glu 240 in TEM-1 are over 6 Å away from the modeled carbenicillin α-carboxylate, suggesting that charge repulsion from these groups likely plays a minor role. This is consistent with mutagenesis experiments in TEM-1 which showed that the E104T and E240G substitutions do not significantly affect k_{cat} and K_m values for the hydrolysis of carboxypenicillins (*24*).

To determine the precise mode of binding of carbenicillin and the relevance of the Ser 130 alternate conformations in PSE-4, a crystal structure of the acyl-enzyme intermediate will be required. Efforts are currently underway to trap the acyl-enzyme intermediate using a deacylation-defective mutant as was accomplished with an E166N TEM-1 mutant (*35*).

ACKNOWLEDGMENT

The authors thank Dr. Y. Luo, R. Pfeutzner, and Dr. S. Mosimann for technical assistance and helpful suggestions. N.C.J.S. is a MRC scholar, a Burroughs Wellcome New Investigator, and a Howard Hughes Medical Institute International Scholar, D.L. is a recipient of a MRC doctoral research award.

REFERENCES

1. Frère, J.-M., Massova, I., and Mobashery, S. (1998) *Antimicrob. Agents Chemother. 42*, 1−17.
2. Medeiros, A. A. (1997) *Clin. Infect. Dis. 24*, S19−S45.
3. Phillipon, A., Dusart, J., Joris, B., and Frère, J.-M. (1998) *Cell. Mol. Life Sci. 54*, 341−346.
4. Boissinot, M., and Levesque, R. C. (1990) *J. Biol. Chem. 256*, 1226−1230.
5. Bodey, G. P., Bolivar, R., Fainstein, V., and Jadeja, L. (1983) *Rev. Infect. Dis. 5*, 279−313.
6. Acred, P., Brown, D. M., Knudsen, E. T., Rolinson, G. N., and Sutherland, R. (1967) *Nature 215*, 25−30.
7. Bush, K., Jacoby, G. A., and Medeiros, A. A. (1995) *Antimicrob. Agents Chemother. 39*, 1211−1233.
8. Matagne, A., Misselyn-Bauduin, A.-M., Joris, B., Erpicum, T., Granier, B., and Frère, J.-M. (1990) *Biochem. J. 265*, 131−146.
9. Lowbury, E. J. L., Kidson, A., Lilly, H. A., Ayliffe, G. A. J., and Jones, R. J. (1969) *Lancet 2*, 448−452.
10. Newsom, S. W. B. (1969) *Lancet 2*, 1141.
11. Newsom, S. W. B., Sykes, R. B., and Richmond, M. H. (1970) *J. Bacteriol. 101*, 1079−1080.
12. Boissinot, M., Huot A., Mercier, J., and Levesque, R. C. (1989) *Mol. Cell. Probes 3*, 179−188.
13. Huovinen, P., and Jacoby, G. A. (1991) *Antimicrob. Agents Chemother. 35*, 2428−2430.
14. Briggs, C. E., and Fratamico, P. M. (1999) *Antimicrob. Agents Chemother. 43*, 846−849.
15. Lachapelle, J., Dufresne, J., and Levesque, R. C. (1991) *Gene 102*, 7−12.
16. Sanschagrin, F., Bejaoui, N., and Levesque, R. C. (1998) *Antimicrob. Agents Chemother. 42*, 1966−1972.
17. Choury, D., Szajnert, M.-F., Joly-Guillou, M.-L., Azibi, K., Delpech, M., and Paul, G. (2000) *Antimicrob. Agents Chemother. 44*, 1070−1074.
18. Choury, D., Aubert, G., Szajnert, M.-F., Azibi, K., Delpech, M., and Paul, G. (1999) *Antimicrob. Agents Chemother. 43*, 297−301.
19. Sakurai, Y., Tsukamoto, K., and Sawai, T. (1991) *J. Bacteriol. 173*, 7038−7041.
20. Ito, Y., and Hirano, T. (1997) *J. Appl. Microbiol. 83*, 175−180.
21. Campbell, J. I., Scahill, S., Gibson, T., and Ambler, R. P. (1989) *Biochem. J. 260*, 803−812.
22. Amber, R. P., Coulson, A. F. W., Frère, J.-M., Ghuysen, J.-M., Joris, B., Levesque, R. C., Tiraby, G., and Waley, S. G. (1991) *Biochem. J. 276*, 269−272.
23. Lenfant, F., Labia, R., and Masson, J.-M. (1991) *J. Biol. Chem. 266*, 17187−17194.
24. Lenfant, F., Petit, A., Labia, R., Maveyraud, L., Samama, J.-P., and Masson, J.-P. (1993) *Eur. J. Biochem. 217*, 936−946.
25. Kunkel, T. A., Roberts, J. D., and Zakour, R. A. (1987). *Methods Enzymol. 154*, 367−82.
26. Jensen, S. E., Westlake, D. W., Wolfe, S. (1982) *J. Antibiot. 35*, 483−490.
27. http://www.expasy.ch/tools/protparam.html.
28. Gill, S. C., and von Hippel, P. H. (1989) *Anal. Biochem.* 182, 319−326.

29. Otwinowski, Z. (1993) *Data Collection and Processing* (Sawyer, L., Isaacs, N., and Bailey, S., Eds.), pp 56−62, SERC, Daresbury Laboratory, Warrington, U.K.
30. Collaborative Computational Project, Number 4. (1994) *Acta Crystallogr., Sect. D 50*, 760−763.
31. Matthews, B. W. (1968) *J. Mol. Biol. 33*, 491−497.
32. Cornish-Bowden, A. (1995) *Analysis of Enzyme Kinetic Data*, pp 3−198, Oxford Science Publications, Oxford University Press, Oxford, U.K.
33. Savoie, A., Sanschagrin, F., Palzkill, T., Voyer, T., and Levesque, R. C. (2000) *Protein Eng. 13*, 267−274.
34. Navaza, J. (1994) *Acta Crystallogr., Sect. A 50*, 157−163.
35. Strynadka, N. C. J., Adachi, H., Jensen, S. E., Johns, K., Sielecki, A., Betzel, C., Sutoh, K., and James, M. N. G. (1992) *Nature 359*, 700−705.
36. Jones, T. A., Zou, J. Y., Cowan, S. W., and Kjeldgaard, M. (1991) *Acta Crystallogr., Sect. A 47*, 110−119.
37. Brünger, A. T., and et al. (1998) *Acta Crystallogr., Sect. D 54*, 905−921.
38. McRee, D. E. (1992) *J. Mol. Graphics 10*, 44−47.
39. Laskowski, R. A., MacArthur, M. W., Moss, D. S., and Thornton, J. M. (1993) *J. App. Crystallogr. 26*, 283−291.
40. Cohen, G. H. (1997) *J. Appl. Crystallogr. 30*, 1160−1161.
41. Dideberg, O., Charlier, P., Wery, J. P., Dehottay, P., Dusart, J., Erpicum, T., Frere, J. M., and Ghuysen, J. M. (1987) *Biochem. J. 245*, 911−913.
42. Swaren, P., Maveyraud, L., Raquet, X., Cabantous, S., Duez, C., Pedelacq, J. D., Mariotte-Boyer, S., Mourey, L., Labia, R., Nicolas-Chanoine, M. H., Nordmann, P., Frere, J. M., and Samama, J. P. (1998) *J. Biol. Chem. 273*, 26714−26721.
43. Ibuka, A., Taguchi, A., Ishiguro, M., Fushinobu, S., Ishii, Y., Kamitori, S., Okuyama, K., Yamaguchi, K., Konno, M, and Matsuzawa, H. (1999) *J. Mol. Biol. 285*, 2079−2087.
44. Kuzin, A. P., Nukaga, M., Nukaga, Y., Hujer, A. M., Bonomo, R. A., and Knox, J. R. (1999) *Biochemistry 38*, 5720−5727.
45. Herzberg, O. (1991) *J. Mol. Biol. 217*, 701−719.
46. Knox, J. R., and Moews, P. C. (1991) *J. Mol. Biol. 220*, 435−55.
47. Swarén, P., Maveyraud, L., Guillet, V., Masson, J.-M., Mourey, L., and Samama, J.-P. (1995) *Structure 3*, 603−613.
48. Lamotte-Brasseur, J., Dive, G., Dideberg, O., Charlier, P., Frere, J.-M., and Ghuysen, J.-M. (1991) *Biochem. J. 279*, 213−221.
49. Jelsch, C., Mourey, L., Masson, J. M., and Samama, J. P. (1993) *Proteins: Struct., Funct., Genet. 16*, 364−383.
50. http://www.ps.toyaku.ac.jp/~dobashi/database/structure/c_group/carbenicillin_sodium.html.
51. Zawadzke, L. E., Chen, C. C., Banerjee, S., Li, Z., Wasch, S., Kapadia, G., Moult, J., and Herzberg, O. (1996) *Biochemistry 35*, 16476−16482.
52. Hedstrom, L. (1996) *Biol. Chem. 377*, 465−470.
53. Petrounia, I. P., and Arnold, F. H. (2000) *Curr. Opin. Biotechnol. 11*, 325−330.
54. Tobin, M. B., Gustafsson, C., and Huisman, G. W. (2000) *Curr. Opin. Struct. Biol. 10*, 421−427.
55. Zaccolo, M., and Gherardi, E. (1999) *J. Mol. Biol. 285*, 775−783.
56. Merrit, E. A., and Murphy, M. E. P. (1994) *Acta Crystallogr., Sect. D 50*, 869−873.
57. Kraulis, P. (1992) *J. Appl. Crystallogr. D24*, 946−950.
58. Honig, B., and Nicholls, A. (1995) *Science 268*, 1144−1149.

BI001653V